On the Formulation of Hybrid Finite-Element and Boundary-Integral Methods for 3-D Scattering

Xin-Qing Sheng, Jian-Ming Jin, *Senior Member, IEEE*, Jiming Song, *Member, IEEE*, Cai-Cheng Lu, *Member, IEEE*, and Weng Cho Chew, *Fellow, IEEE*

***Abstract*— This paper studies, in detail, a variety of formulations for the hybrid finite-element and boundary-integral (FE-BI) method for three-dimensional (3-D) electromagnetic scattering by inhomogeneous objects. It is shown that the efficiency and accuracy of the FE-BI method depends highly on the formulation and discretization of the boundary-integral equation (BIE) used. A simple analysis of the matrix condition number identifies the efficiency of the different FE-BI formulations and an analysis of weighting functions shows that the traditional FE-BI formulations cannot produce accurate solutions. A new formulation is then proposed and numerical results show that the resulting solution has a good efficiency and accuracy and is completely immune to the problem of interior resonance. Finally, the multilevel fast multipole algorithm (MLFMA) is employed to significantly reduce the memory requirement and computational complexity of the proposed FE-BI method.**

***Index Terms*— Boundary-integral equations, electromagnetic scattering, finite-element methods, nonhomogeneous media.**

I. Introduction

THE hybrid finite-element and boundary-integral (FE-BI) method is a powerful numerical technique for computing scattering by inhomogeneous objects. The method first divides the problem into an interior and exterior problem. The field in the interior region is formulated using the finite-element method (FEM) and the field in the exterior region is represented by a boundary-integral equation (BIE). The interior and exterior fields are then coupled by the field continuity conditions.

The hybrid FE-BI method has been first applied to two-dimensional (2-D) scattering problems [1]–[6] and later extended to more challenging three-dimensional (3-D) scattering problems [7]–[14]. To be more specific, Paulsen *et al.* [7] developed the first FE-BI formulation for a general 3-D scattering problem, which employed node-based FEM to discretize the interior fields and used either the electric-field integral equation (EFIE) or the magnetic-field integral equation (MFIE) as BIE to represent the exterior field. The formulation, however, exhibited two major drawbacks. First, it inherited all the difficulties caused by the use of node-based elements to discretize the electric and magnetic fields directly [15]. These difficulties include the treatment of dielectric interfaces and sharp conducting edges and corners and the appearance of spurious solutions. Second, it failed at the interior resonant frequencies, which are defined as the resonant frequencies of a cavity formed by covering the surface where BIE applies with a perfect conductor and filling its interior with the exterior medium. The first difficulty was removed by the use of edge-based FEM [8], [9], [12]–[14] and the second difficulty was alleviated by the use of the combined field integral equation (CFIE), which is a linear combination of EFIE and MFIE [10]–[12], [14].

Although the FE-BI method with the implementation of edge-based elements and CFIE is remarkably more powerful than other numerical techniques in dealing with inhomogeneous objects, it still has a bottleneck, which is the dense matrix generated by BIE. As pointed out in [16], this bottleneck severely limits the capability of the FE-BI method in dealing with large objects. Although this problem can be circumvented in some special problems [9], [16] or partially alleviated using special surfaces to separate the interior and exterior regions [11], [14], no efficient method has been developed for general 3-D problems so far.

Our renewed interest in the FE-BI method originated from the recent development of the fast multipole method (FMM) [17] and the multilevel fast multipole algorithm (MLFMA) [18]. Our objective is to apply MLFMA to BIE to completely remove the bottleneck in the FE-BI method for general 3-D problems. During the course of pursuing this goal, we have encountered several problems associated with the efficiency and accuracy of the FE-BI method implemented using the edge-based elements and CFIE. This paper reports our study of these problems and the implementation of MLFMA in the FE-BI method.

In this paper, we first formulate the general FE-BI method for 3-D scattering problems. We then show that there are several different approaches to the discretization of CFIE, yielding solutions with different efficiency and accuracy. However, none of the traditional approaches produces satisfactory results. The cause is determined and a new formulation is proposed. Furthermore, we show that contrary to the common belief, not all CFIE formulations are immune to the problem of interior resonance; however, the new one is. Finally, we employ MLFMA to significantly reduce the memory requirement and computational complexity of the proposed FE-BI method.

II. Formulation and Analysis

Consider the problem of electromagnetic wave scattering by an arbitrarily-shaped and inhomogeneous body characterized

Manuscript received May 6, 1997; revised October 20, 1997. This work was supported by the Office of Naval Research under Grant N00014-95-1-0848, by a Grant from the Air Force Office of Scientific Research via the MURI Program under Contract F49620-96-1-0025, and by the National Science Foundation under Grant NSF ECE 94-57735.

The authors are with the Center for Computational Electromagnetics, Department of Electrical and Computer Engineering, University of Illinois at Urbana-Champaign, Urbana, IL 61801 USA.

Publisher Item Identifier S 0018-926X(98)02268-6.

0018–926X/98$10.00 © 1998 IEEE

by relative permittivity and permeability (ϵ_r, μ_r), which can be complex if the body is lossy. To solve this problem using the FE-BI method, we first introduce an artificial surface S (which can be the surface of the body) to enclose the body and divide the problem into an interior and an exterior one. The field inside S can be formulated into an equivalent variational problem with the functional given by [15]

$$F(\boldsymbol{E}) = \frac{1}{2}\int_V \left[\frac{1}{\mu_r}(\nabla\times\boldsymbol{E})\cdot(\nabla\times\boldsymbol{E}) - k_0^2\epsilon_r\boldsymbol{E}\cdot\boldsymbol{E}\right] dV + jk_0\int_S (\boldsymbol{E}\times\overline{\boldsymbol{H}})\cdot\hat{n}\, dS \quad (1)$$

where V denotes the volume enclosed by S, $\hat{n}$ denotes the outward unit vector normal to S, k_0 is the free-space wavenumber, and $\overline{\boldsymbol{H}} = Z_0\boldsymbol{H}$ with Z_0 being the free-space intrinsic impedance. Using FEM with edge elements, we obtain the matrix equation

$$\begin{bmatrix} K_{II} & K_{IS} & 0 \\ K_{SI} & K_{SS} & B \end{bmatrix}\begin{Bmatrix} E_I \\ E_S \\ \overline{H}_S \end{Bmatrix} = \begin{Bmatrix} 0 \\ 0 \end{Bmatrix} \quad (2)$$

where $\{E_I\}$ is a vector containing the discrete electric fields inside V, $\{E_S\}$, and $\{\overline{H}_S\}$ are the vectors containing the discrete electric and magnetic fields on S, respectively. Furthermore, $[K_{II}]$, $[K_{IS}]$, $[K_{SI}]$, $[K_{SS}]$, and $[B]$ are sparse matrices and, in particular, $[K_{II}]$ and $[K_{SS}]$ are symmetric and $[K_{IS}] = [K_{SI}]^T$, where the superscript T denotes the transpose.

Equation (2) cannot be solved unless a relation between $\{E_S\}$ and $\{\overline{H}_S\}$ is established. Such a relation is provided by BIE for the exterior field, whose discretization yields

$$[P]\{E_S\} + [Q]\{\overline{H}_S\} = \{b\} \quad (3)$$

where $\{b\}$ is a vector related to the incident field. Combining (2) and (3), we obtain the complete system

$$\begin{bmatrix} K_{II} & K_{IS} & 0 \\ K_{SI} & K_{SS} & B \\ 0 & P & Q \end{bmatrix}\begin{Bmatrix} E_I \\ E_S \\ \overline{H}_S \end{Bmatrix} = \begin{Bmatrix} 0 \\ 0 \\ b \end{Bmatrix} \quad (4)$$

which can be solved for the field inside V and on S.

Whereas the generation of (2) using FEM is standard, the generation of (3) using the method of moments (MoM) can take many different forms. The basic equations for generating (3) are the electric-field integral equation (EFIE) given by

$$\boldsymbol{L}(\overline{\boldsymbol{J}}) - \boldsymbol{K}(\boldsymbol{M}) = \boldsymbol{E}^i \quad (5)$$

and the magnetic-field integral equation (MFIE) given by

$$\boldsymbol{K}(\overline{\boldsymbol{J}}) + \boldsymbol{L}(\boldsymbol{M}) = \overline{\boldsymbol{H}}^i \quad (6)$$

where $\overline{\boldsymbol{J}}$ and $\boldsymbol{M}$ are related to the fields on S by $\overline{\boldsymbol{J}} = \hat{n}\times\overline{\boldsymbol{H}}$ and $\boldsymbol{M} = \boldsymbol{E}\times\hat{n}$, respectively, and $(\boldsymbol{E}^i, \boldsymbol{H}^i)$ denote the incident fields. The operators $\boldsymbol{L}$ and $\boldsymbol{K}$ are defined as

$$\boldsymbol{L}(\boldsymbol{X}) = jk_0\int_S \left[\boldsymbol{X}(\boldsymbol{r}') + \frac{1}{k_0^2}\nabla\nabla'\cdot\boldsymbol{X}(\boldsymbol{r}')\right]G(\boldsymbol{r},\boldsymbol{r}')\, dS' \quad (7)$$

$$\boldsymbol{K}(\boldsymbol{X}) = T\boldsymbol{Y}(\boldsymbol{r}) + \int_S \boldsymbol{X}(\boldsymbol{r}')\times\nabla G(\boldsymbol{r},\boldsymbol{r}')\, dS' \quad (8)$$

where $\boldsymbol{Y}$ is related to $\boldsymbol{X}$ by $\boldsymbol{X} = \hat{n}\times\boldsymbol{Y}$ and

$$G(\boldsymbol{r},\boldsymbol{r}') = \frac{e^{-jk_0R}}{4\pi R} \quad (9)$$

in which $R = |\boldsymbol{r} - \boldsymbol{r}'|$. The bar integral symbol is used to denote a principal value integral and the parameter T is given by $T = 1 - \Omega/4\pi$ where Ω is the solid angle subtended by the observation point [19]. For a smooth surface, $\Omega = 2\pi$ and $T = 1/2$.

Equations (5) and (6) can be discretized by first expanding $\overline{\boldsymbol{J}}$ and $\boldsymbol{M}$ as

$$\overline{\boldsymbol{J}} = \sum_{i=1}^{N_S} \boldsymbol{g}_i\overline{H}_i \quad (10)$$

$$\boldsymbol{M} = \sum_{i=1}^{N_S} \boldsymbol{g}_i E_i \quad (11)$$

where N_S denotes the total number of edges on S and $\boldsymbol{g}_i$ denotes the Rao–Wilton–Glisson (RWG) vector basis functions [20], which are completely compatible with the vector basis functions for the edge elements. Substituting (10) and (11) into (5) and using $\boldsymbol{g}_i$ as the weighting function, we obtain the TE formulation (short for $\hat{t}\cdot\boldsymbol{E}$ where $\hat{t}$ denotes a unit vector tangential to S)

$$[P^{\mathrm{TE}}]\{E_S\} + [Q^{\mathrm{TE}}]\{\overline{H}_S\} = \{b^{\mathrm{TE}}\} \quad (12)$$

where

$$P_{ij}^{\mathrm{TE}} = -\int_S \boldsymbol{g}_i\cdot\boldsymbol{K}(\boldsymbol{g}_j)\, dS \quad (13)$$

$$Q_{ij}^{\mathrm{TE}} = \int_S \boldsymbol{g}_i\cdot\boldsymbol{L}(\boldsymbol{g}_j)\, dS \quad (14)$$

$$b_i^{\mathrm{TE}} = \int_S \boldsymbol{g}_i\cdot\boldsymbol{E}^i\, dS. \quad (15)$$

Similarly, from (6) we obtain the TH formulation (short for $\hat{t}\cdot\boldsymbol{H}$)

$$[P^{\mathrm{TH}}]\{E_S\} + [Q^{\mathrm{TH}}]\{\overline{H}_S\} = \{b^{\mathrm{TH}}\} \quad (16)$$

where

$$P_{ij}^{\mathrm{TH}} = \int_S \boldsymbol{g}_i\cdot\boldsymbol{L}(\boldsymbol{g}_j)\, dS = Q_{ij}^{\mathrm{TE}} \quad (17)$$

$$Q_{ij}^{\mathrm{TH}} = \int_S \boldsymbol{g}_i\cdot\boldsymbol{K}(\boldsymbol{g}_j)\, dS = -P_{ij}^{\mathrm{TE}} \quad (18)$$

$$b_i^{\mathrm{TH}} = \int_S \boldsymbol{g}_i\cdot\overline{\boldsymbol{H}}^i\, dS. \quad (19)$$

Alternatively, we may choose $\hat{n}\times\boldsymbol{g}_i$ as the weighting function and obtain from (5) the NE formulation (short for $\hat{n}\times\boldsymbol{E}$)

$$[P^{\mathrm{NE}}]\{E_S\} + [Q^{\mathrm{NE}}]\{\overline{H}_S\} = \{b^{\mathrm{NE}}\} \quad (20)$$

where

$$P_{ij}^{\mathrm{NE}} = -\int_S \hat{n}\times\boldsymbol{g}_i\cdot\boldsymbol{K}(\boldsymbol{g}_j)\, dS \quad (21)$$

$$Q_{ij}^{\mathrm{NE}} = \int_S \hat{n}\times\boldsymbol{g}_i\cdot\boldsymbol{L}(\boldsymbol{g}_j)\, dS \quad (22)$$

$$b_i^{\mathrm{NE}} = \int_S \hat{n}\times\boldsymbol{g}_i\cdot\boldsymbol{E}^i\, dS \quad (23)$$

and from (6), the NH formulation (short for $\hat{n} \times \boldsymbol{H}$)

$$[P^{NH}]\{E_S\} + [Q^{NH}]\{\overline{H}_S\} = \{b^{NH}\} \tag{24}$$

where

$$P_{ij}^{NH} = \int_S \hat{n} \times \boldsymbol{g}_i \cdot \boldsymbol{L}(\boldsymbol{g}_j)\, dS = Q_{ij}^{\mathrm{NE}} \tag{25}$$

$$Q_{ij}^{NH} = \int_S \hat{n} \times \boldsymbol{g}_i \cdot \boldsymbol{K}(\boldsymbol{g}_j)\, dS = -P_{ij}^{\mathrm{NE}} \tag{26}$$

$$b_i^{NH} = \int_S \hat{n} \times \boldsymbol{g}_i \cdot \overline{\boldsymbol{H}}^i\, dS. \tag{27}$$

Equations (20) and (24) can also be obtained by taking the cross product of $\hat{n}$ with (5) and (6) and then using $\boldsymbol{g}_i$ as the weighting function. (That is the reason we used the abbreviations NE and NH for the two equations.)

Theoretically, any of (12), (16), (20), and (24) can be used as (3). However, each of them suffers from the problem of interior resonance and fails to produce accurate solution at and near certain frequencies corresponding to the resonant frequencies of the cavity formed by covering S with a perfect electric or magnetic conductor and filling it with the exterior medium. To eliminate this problem, one has to combine an equation from EFIE to another equation from MFIE to obtain a combined equation (that is, CFIE) [21]. For example, one can combine (12) with (16) to obtain the TETH formulation or (12) with (24) to obtain the TENH formulation. One can also combine (20) with (16) to obtain the NETH formulation or (20) with (24) to obtain the NENH formulation which is the one employed in [12]. Among the four CFIE combinations, TENH and NETH are used most widely. However, it is not clear which combination would produce the most efficient and accurate solution.

Let us heuristically consider the issue of efficiency first. It is known that the FEM matrices in (4) are diagonally dominant. Hence, (4) would be better conditioned if $[Q]$ is diagonally dominant. An analysis of the matrix property shows that $[P^{\mathrm{NE}}]$ and $[Q^{\mathrm{NH}}]$ are most diagonally dominant, $[Q^{\mathrm{TE}}]$ and $[P^{\mathrm{TH}}]$ are diagonally dominant, and $[P^{\mathrm{TE}}]$, $[Q^{\mathrm{TH}}]$, $[Q^{\mathrm{NE}}]$, and $[P^{\mathrm{NH}}]$ are least diagonally dominant. These facts can be denoted symbolically as

$$[P^{\mathrm{NE}}] = -[Q^{\mathrm{NH}}] \sim \begin{bmatrix} \ddots & & \\ & 2 & \\ & & \ddots \end{bmatrix}$$

$$[Q^{\mathrm{TE}}] = [P^{\mathrm{TH}}] \sim \begin{bmatrix} \ddots & & \\ & 1 & \\ & & \ddots \end{bmatrix}$$

$$[P^{\mathrm{TE}}] = -[Q^{\mathrm{TH}}] \sim \begin{bmatrix} \ddots & & \\ & 0 & \\ & & \ddots \end{bmatrix}$$

$$[Q^{\mathrm{NE}}] = [P^{\mathrm{NH}}] \sim \begin{bmatrix} \ddots & & \\ & 0 & \\ & & \ddots \end{bmatrix}. \tag{28}$$

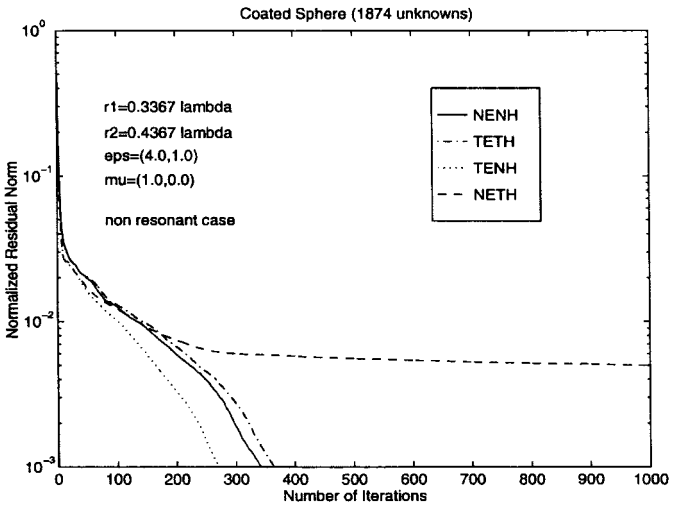

Fig. 1. The normalized residual norm versus the number of iterations in the CG solution of scattering by a coated sphere.

From these, we obtain the matrix structure for the TETH formulation as

$$[P|Q] \sim \left[\begin{array}{ccc|ccc} \ddots & & & \ddots & & \\ & 1 & & & 1 & \\ & & \ddots & & & \ddots \end{array}\right]. \tag{29}$$

For the TENH formulation, we have

$$[P|Q] \sim \left[\begin{array}{ccc|ccc} \ddots & & & \ddots & & \\ & 0 & & & 3 & \\ & & \ddots & & & \ddots \end{array}\right]. \tag{30}$$

For the NETH formulation, we have

$$[P|Q] \sim \left[\begin{array}{ccc|ccc} \ddots & & & \ddots & & \\ & 3 & & & 0 & \\ & & \ddots & & & \ddots \end{array}\right]. \tag{31}$$

Finally, for the NENH formulation, we have

$$[P|Q] \sim \left[\begin{array}{ccc|ccc} \ddots & & & \ddots & & \\ & 2 & & & 2 & \\ & & \ddots & & & \ddots \end{array}\right]. \tag{32}$$

Considering the properties of the FEM matrices in (4), heuristically, it is apparent that the TENH formulation would produce the best conditioned matrix for (4), the NETH formulation would yield the worst conditioned matrix and both TETH and NENH formulations have condition numbers between those of TENH and NETH.

To verify the above predictions, we consider the problem of plane-wave scattering by a coated sphere. The coated sphere has a radius r_2 and its conducting core has a radius r_1. The dielectric coating has a relative permittivity $\epsilon_r = 4$ and a free-space permeability and its thickness is chosen large enough so that there is an appreciable tangential electric field on the surface. Equation (4) is solved using the conjugate gradient (CG) method. Fig. 1 displays the residual norm versus the number of iterations from which we see clearly that TENH

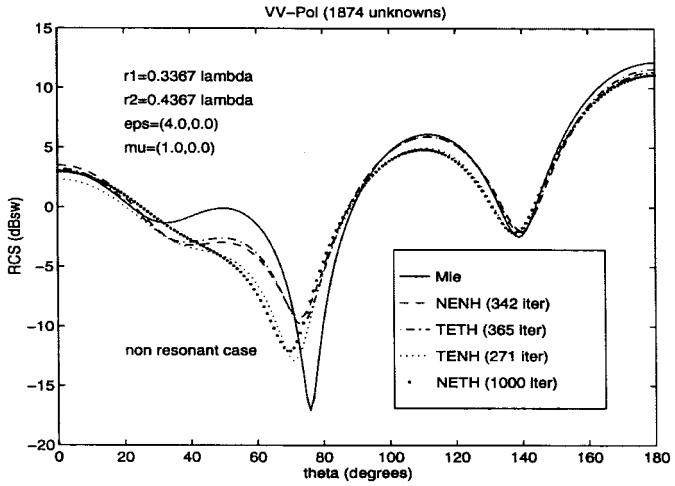

Fig. 2. The bistatic RCS of a coated sphere. Neither of the four formulations produces accurate results.

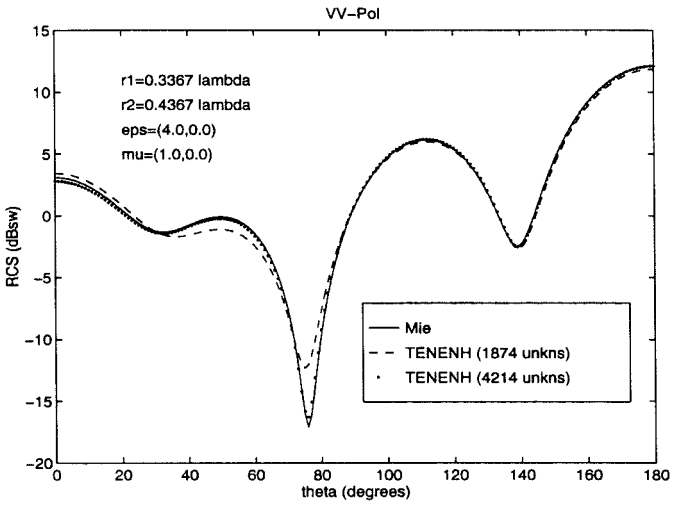

Fig. 3. The bistatic RCS of a coated sphere. Good results are obtained using the TENENH formulation.

converges most quickly, NETH has the worst convergence, and the convergence of TETH and NENH lies between those of TENH and NETH. This observation agrees perfectly with our earlier prediction.

Next, we consider the issue of accuracy. Examining (12)–(27) carefully, we find that in the TE formulation, where $\boldsymbol{g}_i$ is used as the weighting function, the first term in (8) has no contribution to (13) when $i = j$ or, in other words, the first term in (8) is not well tested. The same observation can be made for the TH formulation. However, in the NE formulation, where $\hat{n} \times \boldsymbol{g}_i$ is used as the weighting function, the first term in (7) cannot be tested well and, thus, has no contribution to (22) when $i = j$. The same observation can be made for the NH formulation. Clearly, neither $\boldsymbol{g}_i$ nor $\hat{n} \times \boldsymbol{g}_i$ forms a complete set of weighting function for (5) or (6). Therefore, when $\boldsymbol{g}_i$ or $\hat{n} \times \boldsymbol{g}_i$ is used alone, the solution can become inaccurate unless a very finer discretization is used. Since all the formulations described earlier (TETH, TENH, NETH, and NENH) are the result of using either $\boldsymbol{g}_i$ or $\hat{n} \times \boldsymbol{g}_i$ as the weighting function, their solutions can be inaccurate as well.

The above analysis on accuracy is also verified by the numerical analysis of the problem described earlier. Fig. 2 shows the bistatic radar cross section (RCS) of the coated sphere. It is obvious that all the four formulations have a significant error in their solutions. Our further numerical experiments show that such errors can be reduced by using finer discretization; however, the reduction is insignificant and a finer discretization leads to a much larger number of unknowns. It is interesting to note that both TETH and NENH have a similar error and both TENH and NETH also have a similar error. However, the error in TETH and NENH is smaller than that in TENH and NETH. We note that this problem of inaccuracy occurs only when there exist simultaneously nontrivial tangential electric and magnetic fields on the surface S; therefore, it disappears when one deals with a bare conducting body or a conducting body with a very thin coating where the tangential electric field is very small. We also note that this problem was not observed in [10], [11], and [14] because none of them employed the RWG functions as both the expansion and weighting functions.

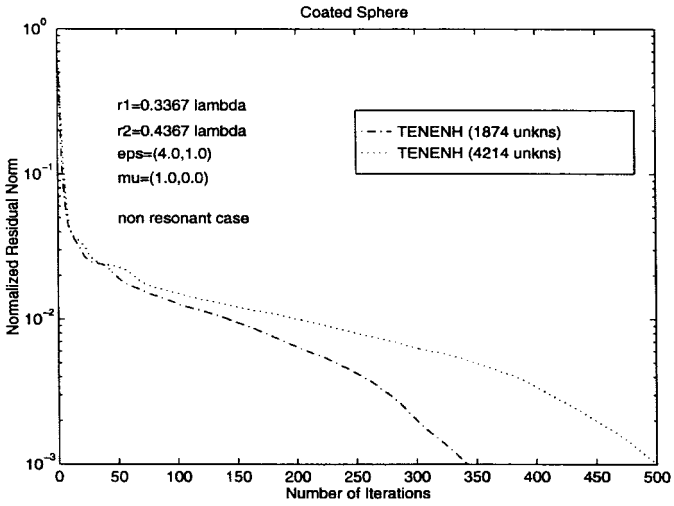

Fig. 4. The normalized residual norm versus the number of iterations for the TENENH formulation.

To alleviate the inaccuracy discussed above, it is clear that a more complete set of weighting functions has to be used. A natural choice is a combination of $\boldsymbol{g}_i$ and $\hat{n} \times \boldsymbol{g}_i$. When this is applied to (5), we obtain a matrix equation, which is equivalent to the sum of (12) and (20) and is referred to as the TENE formulation. When this is applied to (6), we obtain a matrix equation, which is equivalent to the sum of (16) and (24) and is referred to as the THNH formulation. However, since TENE comes from EFIE and THNH comes from MFIE, both would suffer from the problem of interior resonance. One remedy is to combine TENE and THNH. A more efficient alternative is to combine TENE with either the NH or TH formulation. A simple analysis of matrix condition shows that among NH and TH, NH is a better choice for the combination with TENE. Fig. 3 shows the result of TENENH from which we see that TENENH has a significantly better accuracy than those in Fig. 2. The remaining error in TENENH can be reduced by using a finer discretization. The corresponding convergence curves are given in Fig. 4.

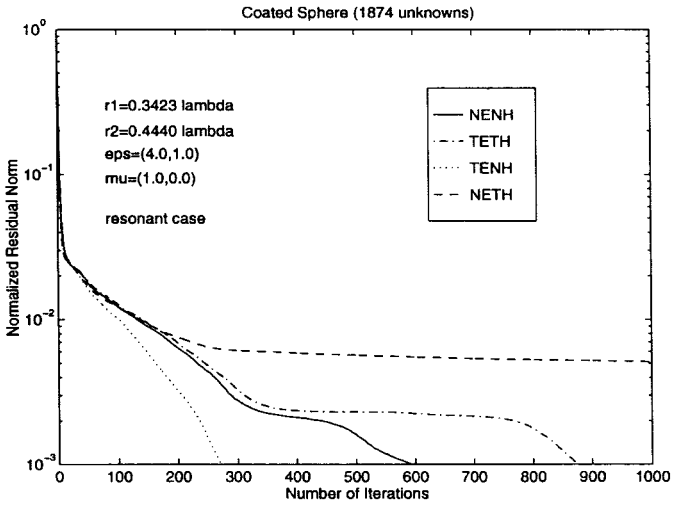

Fig. 5. The normalized residual norm versus the number of iterations in the CG solution of scattering by a coated sphere at a frequency of interior resonance.

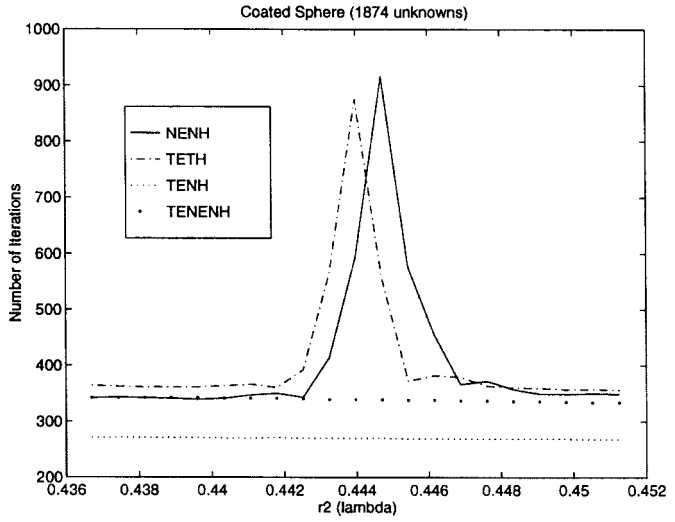

Fig. 6. The number of iterations versus frequency (equivalently, the size of the scatterer in terms of wavelength). Both NENH and TETH exhibit singular behavior near the frequency of interior resonance whereas both TENH and TENENH display a stable behavior.

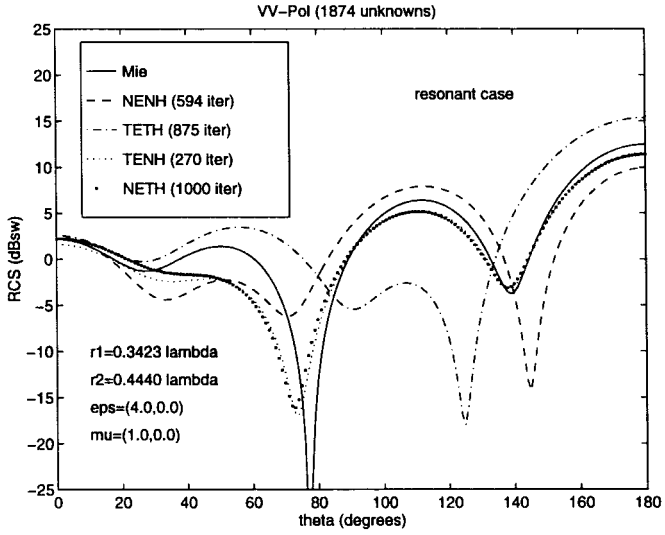

Fig. 7. The bistatic RCS of a coated sphere at a frequency of interior resonance. Neither of the four formulations produces accurate results. In particular, both NENH and TETH yield erroneous results.

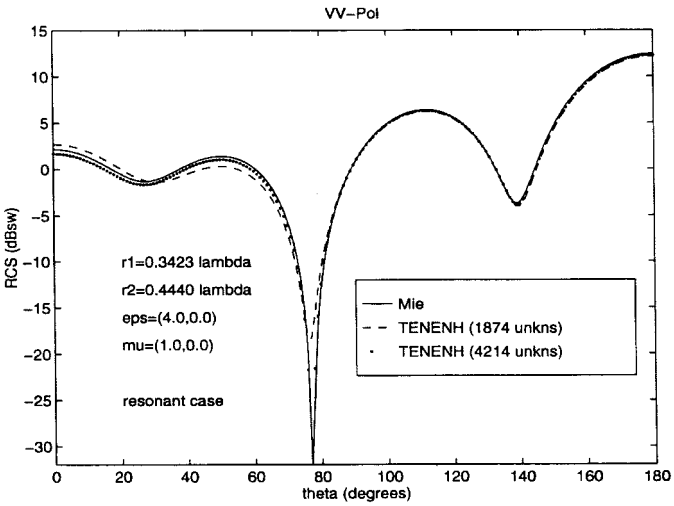

Fig. 8. The bistatic RCS of a coated sphere at a frequency of interior resonance. Again, good results are obtained using the TENENH formulation.

The results presented above are obtained at a frequency that does not coincide with a frequency of interior resonance. To ensure the validity of our analysis, we consider the same coated sphere at a frequency of interior resonance. Fig. 5 displays the residual norm versus the number of iterations from which we observe a similar convergence behavior that agrees with our prediction. However, compared to Fig. 1, the number of iterations for TETH and NENH in this case has increased significantly whereas that for TENH and NETH remains the same. To investigate this problem further, we recorded the number of iterations at the frequencies near the frequency of interior resonance and the result is given in Fig. 6. To our surprise, both TETH and NENH have a sharp peak at the frequency of interior resonance. This implies that both TETH and NENH yield an ill-conditioned matrix and still suffer from the problem of interior resonance, although they are derived from the CFIE formulation.[1] However, the bandwidth of the ill-conditioned peaks is extremely narrow (less than 1%), compared to those resulting from either the EFIE or the MFIE (about 10%) and this is probably the reason that this problem was not detected before. The results for the RCS are given in Fig. 7. As expected, both TETH and NENH yield a result drastically different from the exact solution, whereas both TENH and NETH produce a stable result with an error similar to that in Fig. 2. The result obtained using TENENH is presented in Fig. 8 from which a good agreement is observed. The number of iterations at the frequencies near the frequency of interior resonance is also given in Fig. 6, showing a very stable behavior.

[1]It is well known that CFIE removes the interior resonance by combining EFIE and MFIE in such a manner that the resultant integral operators correspond to that for a cavity with a resistive wall. The proper combinations are TENH and NETH. Both TETH and NENH are the improper combinations in the sense that the combined integral operators do not correspond to those for a resistive cavity and, therefore, they still experience the interior resonance.

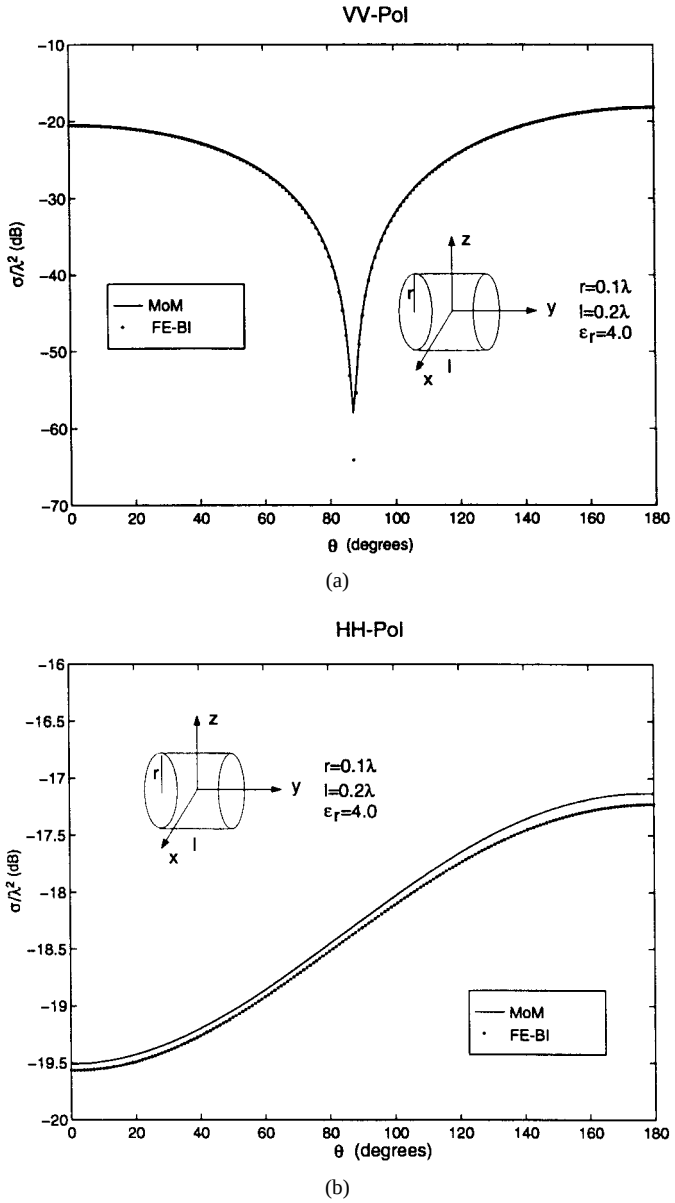

Fig. 9. The bistatic RCS of a finite dielectric cylinder in the x-z plane for a plane wave incident along the z axis. (a) VV-polarization. (b) HH-polarization.

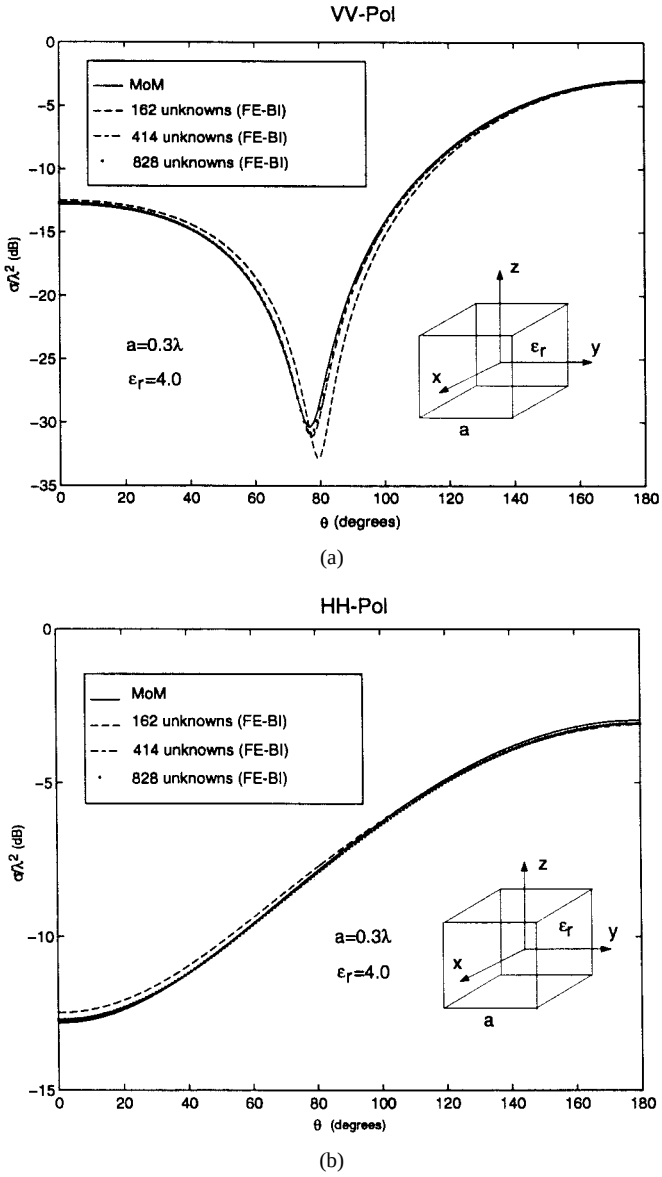

Fig. 10. The bistatic RCS of a dielectric cube in the x-z plane for a plane wave incident along the z-axis. (a) VV-polarization. (b) HH-polarization.

Next, we present several other examples to demonstrate the accuracy and capability of the proposed formulation for other geometries. Fig. 9 shows the bistatic RCS of a finite dielectric cylinder and Fig. 10 displays the result for a dielectric cube. All the results are compared with those obtained from MoM and excellent agreement is observed in each case. We note that the MoM solutions shown in Figs. 9 and 10 are obtained from the Poggio–Miller–Chang–Harrington–Wu (PMCHW) formulation [22], which is a combined-source integral equation (CSIE). The PMCHW formulation is known to produce an accurate solution [23], [24]; however, it can be applied to only homogeneous objects.

III. Application of MLFMA

As pointed out in [16], the FE-BI method has a bottleneck which is the dense matrix generated by BIE. This bottleneck severely limits the capability of the FE-BI method in dealing with large objects since the dense matrices $[P]$ and $[Q]$ have a memory requirement of $O(N_S^2)$ and a computational complexity of $O(N_S^2)$ to compute a matrix-vector product.

One solution to the problem discussed above is to compute the matrix-vector products using fast multipole method (FMM) [17]. The basic idea of FMM is first to divide the surface subscatterers into groups. The addition theorem is then used to translate the scattered field of different scattering centers within a group into a single center and this process is called aggregation. Doing this, the number of scattering centers is reduced significantly. Similarly, for each group the field scattered by all the other group centers can be first received by the group center and then redistributed to the subscatterers belonging to the group. This process is called disaggregation. It has been shown that FMM can reduce the memory requirement and computational complexity to $O(N_S^{1.5})$.

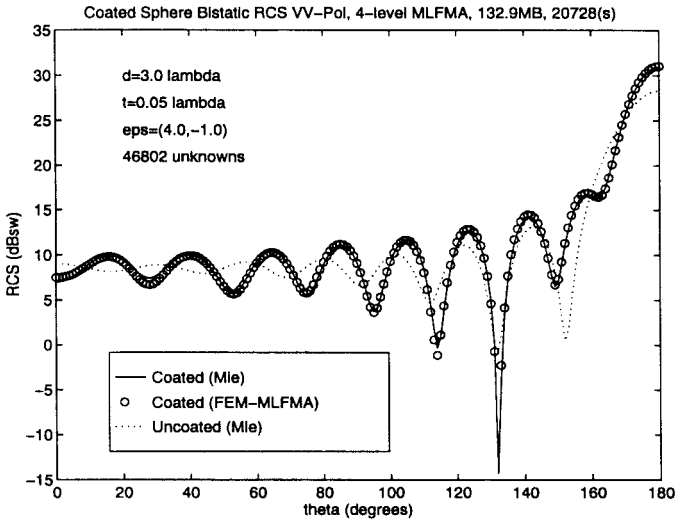

(a)

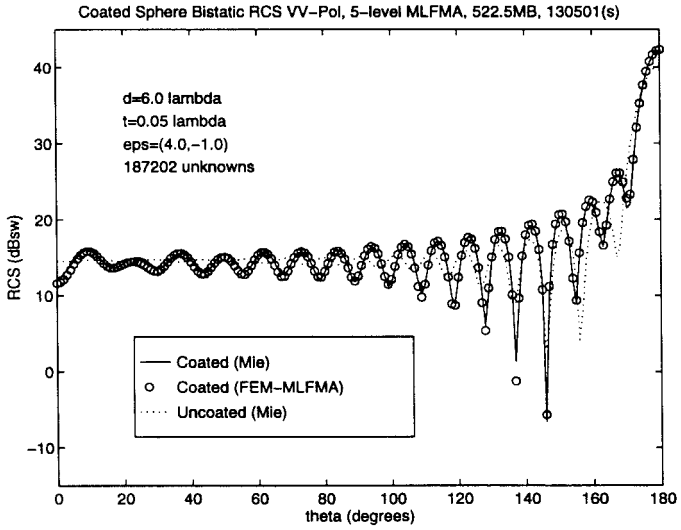

(b)

Fig. 11. The bistatic RCS of a coated sphere. The conducting sphere has a diameter d and the coating has a thickness $t = 0.05\lambda_0$, a relative permittivity $\epsilon_r = 4.0 - j1.0$, and a relative permeability $\mu_r = 1$. (a) $d = 3\lambda_0$. (b) $d = 6\lambda_0$.

The memory requirement and computational complexity can be further reduced to $O(N_S \log N_S)$ using MLFMA [18]. To implement MLFMA, the entire object is first enclosed in a large cube, which is divided into eight smaller cubes. Each subcube is then recursively subdivided into smaller cubes until the edge length of the finest cube is about half a wavelength. For two points in the same or nearby finest cubes, their interaction is calculated in a direct manner. However, when the two points reside in different nonnearby cubes, their interaction is calculated by FMM, as described above. The level of cubes on which FMM is applied depends on the distance between the two points. The detailed description of MLFMA is given in [18] and is not repeated here, although the equations to be treated are different.

The basic formulas derived with the addition theorem to calculate the matrix elements for nonnearby groups, are given

TABLE I
MEMORY REQUIREMENT AND CPU TIME FOR THE FEM-MLFMA SOLUTION OF SCATTERING FROM A COATED SPHERE

Sphere diameter	Number of unknowns	Level of MLFMA	Memory requirement	CPU time per iteration	Total CPU time
$0.75\lambda_0$	3,330	2	14.7 MB	0.424 s	683 s
$1.5\lambda_0$	11,704	3	37.6 MB	3.343 s	3,750 s
$3\lambda_0$	46,802	4	132.9 MB	18.46 s	20,728 s
$6\lambda_0$	187,202	5	522.5 MB	87.84 s	130,501 s

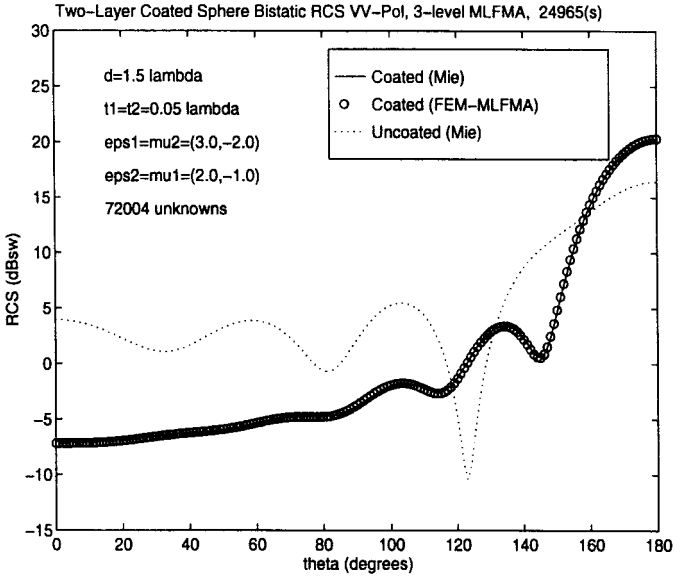

Fig. 12. The bistatic RCS of a sphere coated with two dielectric layers. The conducting sphere has a diameter $d = 1.5\lambda_0$, the inner layer has a thickness $t_1 = 0.05\lambda_0$, a relative permittivity $\epsilon_{r1} = 3.0 - j2.0$, and a relative permeability $\mu_{r1} = 2.0 - j1.0$, and the outer layer has a thickness $t_2 = 0.05\lambda_0$, a relative permittivity $\epsilon_{r2} = 2.0 - j1.0$, and a relative permeability $\mu_{r2} = 3.0 - j2.0$.

by

$$P_{ij} = \left(\frac{k_0}{4\pi}\right)^2 \oint \boldsymbol{V}_{im}^P T_{mm'}(\hat{k}\cdot\hat{r}_{mm'})\cdot \boldsymbol{V}_{jm'} d^2\hat{k} \tag{33}$$

$$Q_{ij} = \left(\frac{k_0}{4\pi}\right)^2 \oint \boldsymbol{V}_{im}^Q T_{mm'}(\hat{k}\cdot\hat{r}_{mm'})\cdot \boldsymbol{V}_{jm'} d^2\hat{k} \tag{34}$$

where

$$\boldsymbol{V}_{im}^P = \int_S e^{-j\boldsymbol{k}_0\cdot\boldsymbol{r}_{im}}[\alpha_1\hat{k}\times\boldsymbol{g}_i + \alpha_2\hat{k}\times\hat{n}\times\boldsymbol{g}_i + \alpha_3(\overline{\boldsymbol{I}} - \hat{k}\hat{k})\cdot(\hat{n}\times\boldsymbol{g}_i)]\, dS \tag{35}$$

$$\boldsymbol{V}_{im}^Q = \int_S e^{-j\boldsymbol{k}_0\cdot\boldsymbol{r}_{im}}[(\overline{\boldsymbol{I}} - \hat{k}\hat{k})\cdot(\alpha_1\boldsymbol{g}_i + \alpha_2\hat{n}\times\boldsymbol{g}_i) - \alpha_3\hat{k}\times\hat{n}\times\boldsymbol{g}_i]\, dS \tag{36}$$

$$V_{jm'} = \int_S e^{j\boldsymbol{k}_0\cdot\boldsymbol{r}_{jm'}}\boldsymbol{g}_j\, dS \tag{37}$$

and

$$T_{mm'}(\hat{k}\cdot\hat{r}_{mm'}) = \sum_{l=0}^{L}(-j)^l(2l+1)h_l^{(2)}(k_0 r_{mm'})\cdot P_l(\hat{r}_{mm'}\cdot\hat{k}). \tag{38}$$

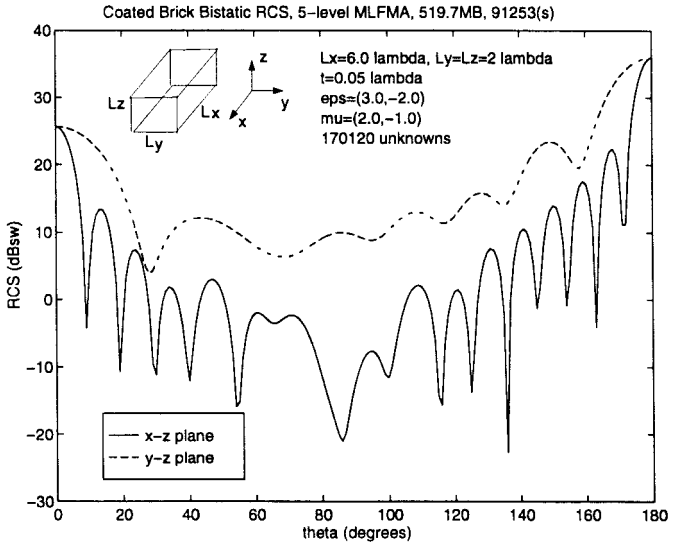

Fig. 13. The bistatic RCS of a coated brick for a plane wave incident along the z axis from the top with the incident electric field in the x-z plane. The conducting brick has a size $6\lambda_0 \times 2\lambda_0 \times 2\lambda_0$ and the coating has a thickness $t = 0.05\lambda_0$, a relative permittivity $\epsilon_r = 3.0 - j2.0$, and a relative permeability $\mu_r = 2.0 - j1.0$.

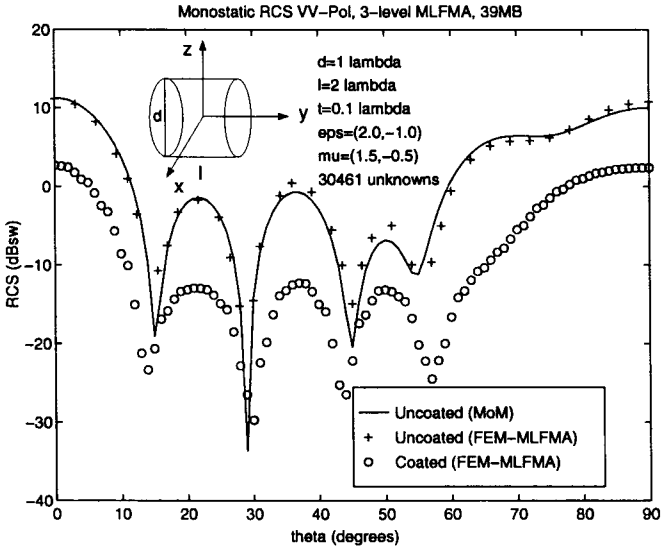

Fig. 14. The monostatic RCS of a coated finite cylinder in the y-z plane. The conducting cylinder has a diameter $d = 1.0\lambda_0$ and a length $l = 2.0\lambda_0$ and the coating has a thickness $t = 0.1\lambda_0$, a relative permittivity $\epsilon_r = 2.0 - j1.0$, and a relative permeability $\mu_r = 1.5 - j0.5$.

In the above, the integrals in (33) and (34) are over the unit spherical surface, $\boldsymbol{g}_i$ resides in a group G_m centered at $\boldsymbol{r}_m$, $\boldsymbol{g}_j$ resides in a group $G_{m'}$ centered at $\boldsymbol{r}_{m'}$, $\boldsymbol{r}_{im} = \boldsymbol{r}_i - \boldsymbol{r}_m$, $\boldsymbol{r}_{jm'} = \boldsymbol{r}_j - \boldsymbol{r}_{m'}$, and $\boldsymbol{r}_{mm'} = \boldsymbol{r}_m - \boldsymbol{r}_{m'}$. The α_1, α_2, and α_3 in (35) and (36) are the combination parameters in the TENENH formulation. Also in (38), $h_l^{(2)}$ denotes the spherical Hankel function of the second kind, P_l denotes the Legendre polynomial of degree l, and L denotes the number of multipole expansion terms whose choice is discussed in [18].

As described earlier, MLFMA converts the direct interaction component P_{ij} or Q_{ij} between two "far-away" points i and j into three indirect components: 1) the radiation component from the point j to the group center m', which is represented by $\boldsymbol{V}_{jm'}$; 2) the translation component from the group center m' to another group center m, represented by $T_{mm'}$; and 3) the receiving component from the group center m to the point i, which is represented by $\boldsymbol{V}_{im}$. Among these three components, only the receiving component is different for different formulations—the other two components, the translation, and the radiation components are the same.

The MLFMA described above is implemented for the solution of the proposed FE-BI formulation. The combination parameters used are $\alpha_1 = \alpha_2 = 0.45$ and $\alpha_3 = 0.1$. Fig. 11 shows the bistatic RCS of a conducting sphere having a diameter d and coated with a lossy dielectric layer having a thickness t. The results are compared to those obtained using the Mie series and good agreement is observed. The memory requirement and the total CPU time on one processor of an SGI Power Challenge (R8000) are given in Table I. These results are obtained without using a preconditioner. Fig. 12 shows the result for a sphere coated with two dielectric layers. Finally, Figs. 13 and 14 give two additional examples: one for a coated conducting brick and the other for a coated finite cylinder.

IV. Conclusion

In this paper, we studied in detail a variety of formulations for the hybrid FE-BI method for calculating 3-D electromagnetic scattering by inhomogeneous objects. We showed that the efficiency and accuracy of the FE-BI method depend highly on the formulation and discretization of BIE used. We considered four formulations (TETH, TENH, NETH, and NENH) obtained from the discretization of the CFIE and we found the following from analysis (and it was verified numerically).

- TENH produces the best conditioned FE-BI matrix equation and NETH produces the worst conditioned matrix equation. Therefore, when an iterative solver such as the CG algorithm is employed to solve the matrix equation, TENH is the most efficient formulation.
- None of the four formulations produces accurate FE-BI solutions because neither the RWG vector basis functions $(\boldsymbol{g}_i)$ nor its cross product with the unit normal $(\hat{n} \times \boldsymbol{g}_i)$ form a complete set of weighting functions for EFIE or MFIE on a general surface where nontrivial equivalent electric and magnetic currents exist simultaneously.
- Both TETH and NENH suffer from the problem of interior resonance although the bandwidth of the bad solution is extremely narrow compared to those resulting from EFIE and MFIE. However, TENH and NETH are immune to the problem of interior resonance although their results are inaccurate.

Based on the analysis, we proposed a formulation (TENENH) that has a good efficiency and a good accuracy and is completely immune to the corruption of interior resonance. The TENE part of this formulation is equivalent to testing the pertinent EFIE by $\boldsymbol{g}_i + \hat{n} \times \boldsymbol{g}_i$. We then applied MLFMA to the proposed FE-BI method to enhance its capability to deal with larger objects.

REFERENCES

[1] S. P. Marin, "Computing scattering amplitudes for arbitrary cylinders under incident plane waves," *IEEE Trans. Antennas Propagat.*, vol. AP-30, pp. 1045–1049, Nov. 1982.

[2] J. M. Jin and V. V. Liepa, "Application of hybrid finite element method to electromagnetic scattering from coated cylinders," *IEEE Trans. Antennas Propagat.*, vol. 36, pp. 50–54, Jan. 1988.

[3] ——, "A note on hybrid finite element method for solving scattering problems," *IEEE Trans. Antennas Propagat.*, vol. 36, pp. 1486–1490, Oct. 1988.

[4] Z. Gong and A. W. Glisson, "A hybrid equation approach for the solution of electromagnetic scattering problems involving two-dimensional inhomogeneous dielectric cylinders," *IEEE Trans. Antennas Propagat.*, vol. 38, pp. 60–68, Jan. 1990.

[5] K. L. Wu, G. Y. Delisle, D. G. Fang, and M. Lecours, "Coupled finite element and boundary element methods in electromagnetic scattering," in *Finite Element and Finite Difference Methods in Electromagnetic Scattering*. New York: Elsevier, 1990.

[6] X. Yuan, D. R. Lynch, and J. W. Strohbehn, "Coupling of finite element and moment methods for electromagnetic scattering from inhomogeneous objects," *IEEE Trans. Antennas Propagat.*, vol. 38, pp. 386–393, Mar. 1990.

[7] K. D. Paulsen, D. R. Lynch, and J. W. Strohbehn, "Three-dimensional finite, boundary, and hybrid element solutions of the Maxwell equations for lossy dielectric media," *IEEE Trans. Microwave Theory Tech.*, vol. 36, pp. 682–693, Apr. 1988.

[8] X. Yuan, "Three-dimensional electromagnetic scattering from inhomogeneous objects by the hybrid moment and finite element method," *IEEE Trans. Microwave Theory Tech.*, vol. 38, pp. 1053–1058, Aug. 1990.

[9] J. M. Jin and J. L. Volakis, "A hybrid finite element method for scattering and radiation by microstrip patch antennas and arrays residing in a cavity," *IEEE Trans. Antennas Propagat.*, vol. 39, pp. 1598–1604, Nov. 1991.

[10] J.-J. Angelini, C. Soize, and P. Soudais, "Hybrid numerical method for harmonic 3-D Maxwell equations: Scattering by a mixed conducting and inhomogeneous anisotropic dielectric medium," *IEEE Trans. Antennas Propagat.*, vol. 41, pp. 66–76, May 1993.

[11] W. E. Boyes and A. A. Seidl, "A hybrid finite element method for 3-D scattering using nodal and edge elements," *IEEE Trans. Antennas Propagat.*, vol. 42, pp. 1436–1442, Oct. 1994.

[12] G. E. Antilla and N. G. Alexopoulos, "Scattering from complex three-dimensional geometries by a curvilinear hybrid finite-element integral-equation approach," *J. Opt. Soc. Amer. A*, vol. 11, no. 4, pp. 1445–1457, Apr. 1994.

[13] T. Eibert and V. Hansen, "Calculation of unbounded field problems in free space by a 3-D FEM/BEM-hybrid approach," *J. Electromagn. Waves Appl.*, vol. 10, no. 1, pp. 61–77, 1996.

[14] T. Cwik, C. Zuffada, and V. Jamnejad, "Modeling three-dimensional scatterers using a coupled finite element–integral equation formulation," *IEEE Trans. Antennas Propagat.*, vol. 44, pp. 453–459, Apr. 1996.

[15] J. M. Jin, *The Finite Element Method in Electromagnetics*. New York: Wiley, 1993.

[16] N. Lu and J. M. Jin, "Application of fast multipole method to finite-element boundary-integral solution of scattering problems," *IEEE Trans. Antennas Propagat.*, vol. 44, pp. 781–786, June 1996.

[17] R. Coifman, V. Rokhlin, and S. Wandzura, "The fast multipole method for the wave equation: A pedestrian prescription," *IEEE Trans. Antennas Propagat. Mag.*, vol. 35, pp. 7–12, June 1993.

[18] J. M. Song and W. C. Chew, "Multilevel fast-multipole algorithm for solving combined field integral equations of electromagnetic scattering," *Microwave Opt. Tech. Lett.*, vol. 10, no. 1, pp. 14–19, Sept. 1995.

[19] A. J. Poggio and E. K. Miller, "Integral equation solutions of three dimensional scattering problems," in *Computer Techniques for Electromagnetics*. Oxford, U.K.: Permagon, 1973, ch. 4.

[20] S. M. Rao, D. R. Wilton, and A. W. Glisson, "Electromagnetic scattering by surfaces of arbitrary shape," *IEEE Trans. Antennas Propagat.*, vol. AP-30, pp. 409–418, May 1982.

[21] S. M. Rao and D. R. Wilton, "E-field, H-field, and combined field solution for arbitrarily shaped three-dimensional dielectric bodies," *Electromagn.*, vol. 10, no. 4, pp. 407–421, 1990.

[22] J. R. Mautz and R. F. Harrington, "Electromagnetic scattering from a homogeneous material body of revolution," *Arch. Elektron. Übertragungstech.*, vol. 33, pp. 71–80, 1979.

[23] L. N. Medgyesi-Mitschang, J. M. Putnam, and M. B. Gedera, "Generalized method of moments for three-dimensional penetrable scatterers," *J. Opt. Soc. Amer. A*, vol. 11, no. 4, pp. 1383–1398, Apr. 1994.

[24] S. M. Rao, C. C. Cha, R. L. Cravey, and D. Wilkes, "Electromagnetic scattering from arbitrary shaped conducting bodies coated with lossy materials of arbitrary thickness," *IEEE Trans. Antennas Propagat.*, vol. 39, pp. 627–631, May 1991.

Xin-Qing Sheng was born in Anhui, China, in 1968. He received the B.S., M.S., and Ph.D. degrees from the University of Science and Technology of China (USTC), Hefei, China, in 1991, 1994, and 1996, respectively.

Since April 1996, he has been a Postdoctoral Research Fellow in the Center for Computational Electromagnetics, Department of Electrical and Computer Engineering, University of Illinois at Urbana-Champaign. He has published over 25 papers in academic journals and conference proceedings. His research interests include computational electromagnetics, radar cross-section analysis, and the analysis of microwave and millimeter-wave transmission problems.

Dr. Sheng is a recipent of the 1995 President Award of the Chinese Academy of Science.

Jian-Ming Jin (S'87–M'89–SM'94) received the B.S. and M.S. degrees in applied physics from Nanjing University, Nanjing, China, in 1982 and 1984, respectively, and the Ph.D. degree in electrical engineering from the University of Michigan, Ann Arbor, in 1989.

In 1993, he joined the faculty of the Department of Electrical and Computer Engineering at the University of Illinois at Urbana-Champaign (UIUC) after working as a Senior Scientist at Otsuka Electronics, Inc., Fort Collins, CO. From 1982 to 1985 he was associated with the Department of Physics of Nanjing University, Nanjing, China, where he started his research on the application of the finite-element method to electromagnetics problems. He continued this research at the University of Michigan, Ann Arbor, where he was first a Research Assistant, then a Research Fellow, and in 1990 was appointed as an Assistant Research Scientist. Currently, he is an Associate Professor of Electrical and Computer Engineering and Associate Director of the Center for Computational Electromagnetics at UIUC. He is a member of the Editorial Board of the *Electromagnetics Journal*. He has published over 50 articles in refereed journals and several book chapters. He authored *The Finite Element Method in Electromagnetics* (New York: Wiley, 1993) and co-authored *Computation of Special Functions* (New York: Wiley, 1996). His current research interests include computational electromagnetics, scattering and antenna analysis, electromagnetic compatibility, and magnetic resonance imaging.

Dr. Jin is a member of Commision B of USNC/URSI and Tau Beta Pi. He is a recipient of the 1994 National Science Foundation Young Investigator Award and the 1995 Office of Naval Research Young Investigator Award. He also received a 1997 Junior Xerox Research Award from UIUC College of Engineering. He serves as an Associate Editor of the IEEE TRANSACTIONS ON ANTENNAS AND PROPAGATION.

Jiming Song (S'92–M'95), for photograph and biography, see p. 245 of the February 1997 issue of this TRANSACTIONS.

Cai-Cheng Lu (S'93–M'95), for photograph and biography, see p. 543 of the March 1997 issue of this TRANSACTIONS.

Weng Cho Chew (S'79–M'80–SM'86–F'93), for photograph and biography, see p. 245 of the February 1997 issue of this TRANSACTIONS.